Available online at www.sciencedirect.com
SCIENCE DIRECT®
Journal of Crystal Growth 264 (2004) 400–408
JOURNAL OF CRYSTAL GROWTH
www.elsevier.com/locate/jcrysgro

Syntheses and structures of sodium aluminodiphosphonates with different morphologies (diphosphonate = 1-hydroxyethylidenediphosphonate) ☆

Zongbin Wu[a], Zhongmin Liu[a,*], Peng Tian[a], Yue Yang[a], Lei Xu[a], Haibin Song[b], Xinhe Bao[c], Xiumei Liu[c], Xianchun Liu[c]

[a] *Natural Gas Utilization, Applied Catalysis Laboratory, Dalian Institute of Chemical Physics, Chinese Academy of Sciences, P. O. Box 110, Dalian 116023, People's Republic of China*
[b] *State Key Laboratory of Elemento-Organic Chemistry, Nankai University, Tianjin 300071, People's Republic of China*
[c] *State Key Laboratory of Catalysis, Dalian Institute of Chemical Physics, Chinese Academy of Sciences, P. O. Box 110, Dalian 116023, People's Republic of China*

Received 4 November 2003; accepted 16 December 2003
Communicated by M. Uwaha

Abstract

A new family of sodium aluminodiphosphonates (diphosphonate = 1-hydroxyethylidenediphosphonate) has been synthesised hydrothermally at 433 K for 15 days. By altering the aluminium source, two different morphologies, namely hexagonal tubular and solid morphology, have been obtained, and the corresponding crystals were named as DLES-Alt and DLES-Als, respectively. Under the synthesis condition for DLES-Alt, if the reaction time was changed to 7 days, a small amount of crystals with the solid morphology accompanying DLES-Alt were observed, and designated as DLES-Alts. Meanwhile, crystals with a plate-like morphology (designated as DLES-Alp) were always the accompanying phase of the main phase of DLES-Alt or DLES-As. All of the crystals were isostructures. A hexagonal ring containing a propeller-like chiral motif along [0 0 1] is a common characteristic of these crystals. Being a representative case, the crystallographic data of DLES-Alt is trigonal (space group P-3), with cell parameters at 293 K as follows: $a = 17.853(4)$, $b = 17.853(4)$, $c = 8.823(4)$ Å, $V = 2435.3(14)$ Å^3, and $Z = 6$.

PACS: 81.10; 81.10.A

Keywords: A1. Crystal morphology; A1. Crystal structure; A2. Hydrothermal crystal growth

1. Introduction

The relationships among composition, structure and property are important issues in the field of materials. Recent interest in syntheses of nanomaterials and novel materials with anisotropic

☆ Supplementary data associated with this article can be found at doi:10.1016/j.jcrysgro.2003.12.023

*Corresponding author. Tel.: +864114685510; fax: +864114691570.
E-mail address: liuzm@dicp.ac.cn (Z. Liu).

0022-0248/$ - see front matter © 2004 Elsevier B.V. All rights reserved.
doi:10.1016/j.jcrysgro.2003.12.023

morphologies renders new impetus to the domain of synthetic materials [1–5]. Up to now, numerous researches involving the effects of decreasing particle size of a material on its properties have been reported. However, investigations concerning man-made materials with anisotropic morphology and their formation mechanisms are just at an initial stage. In this paper, we are focusing on the investigation of tubular morphology, because this morphology is a representative one in the family of anisotropic morphologies.

After the reporting of the tubular crystal of natural chrysotile asbestos [6], the field of synthetic materials with geometrically closed structures has long been dominated by carbon systems [7]. Recently, researches in this field have resulted in the formation of some novel materials that possess tubular morphologies, including both organic [3] and inorganic materials (carbon tube [7], MCM-41 [8], vanadium oxide [9], titanium oxide [10], nickelous chloride [11], transition metal oxychlorides [12], tungsten oxide [13], Sr–Er–Sialon and Sr–Dy–Sialon [14], B–C–N, C–N and B–N systems [15], metallic crystals like Cu–Sn–Ge alloy, Gu_3Ge and $[Sn_6O_8Ge(NH_3)]_n$ [16], and several chalcogenides [17–23]). In opposition to the abundant nanotubes, up to now, only a few tubular crystalline materials in millimetre-scale have been reported [12,13,19–24] and all of them are just known crystals showing new morphologies.

There are many proposed mechanisms on the growth of tubular crystals, such as the liquid-crystal phase transformation mechanism [8], the organogel template-directed mechanism [9], the VLS or/and VS mechanism (VLS = vapour liquid solid) [14], the mechanism involving "contaminating atoms" proposed by Tenne [18], the heat transfer mechanism [12,20], the wrapping of sheets of layered compounds [19,24], the base growth and tip growth mechanism [25,26], and so on. All of these mechanisms have limited applications, as their formulations are based on specific materials that the authors were studying. Therefore, in order to form an intrinsic growth mechanism, many theoretical and experimental explorations should be done in a planned way.

Although reported inorganic tubular crystals possess different composition and size, they usually exhibit lamellar structures, and most of them have slight misfits between the sheets. This idea was first put forward by Betas et al. [6], and strengthened by Patzke et al. [2]. Furthermore, Patzke et al. predicted that in principle all layered materials should be transformable into tubular morphologies under suitable reaction conditions. It is known that many inorganic–organic hybrids have lamellar structures [27–29]. The fact implies that inorganic–organic hybrids would be potential sources for preparing novel tubular materials.

Our synthesis strategy for achieving inorganic–organic hybrid tubular crystals involved the use of 1-hydroxyethylidenediphosphonate (hedp) for introducing organic components into the structure, and employment of the hydrothermal method for realising crystallisation. 1-hydroxyethylidenediphosphonic acid (H_4hedp), featuring a P–C–P linkage, has versatile coordination abilities with metal ions [30–33]. Because of the presence of seven active oxygen atoms, hedp anions can function as bi-, tri-, tetra-, penta-, or hexadentate ligands. Furthermore, the $-CH_3$ and $-OH$ groups attached to the organic tether may provide a steric hindrance on the one hand, and offer a hydrophobic or hydrophilic environment on the other hand. More recently, great efforts have been devoted to the synthesis of metal-hedp compounds with open-framework. The idea was highlighted by the study of Sn_2(hedp) [34]. In such a compound, the linkage of the two fundamental structural motif of $\{SnO_3\}$ and $\{O_3PC\}$ produces eight or 16 member rings, which connect in turn to form open-channels paralleling to the *a*- or *c*-axis. Attempting to obtain novel structures, Zheng et al. synthesised several new metal-hedp compounds by using different kinds of organic amines as templates [32,35]. They attributed the structural differences among the compounds to the effects of the employed templates. The smaller sized template, $NH_2CH_2CH_2NH_2$, could direct to the formation of a linear single chain compound, whereas the larger sized templates of $NH_2(CH_2)_mNH_2$ ($m = 4, 5, 6$) could lead to the formation of anionic double chains holding together by strong hydrogen bonds to form two or three-dimensional structures. In addition, Zheng et al. reported two metal-hedp compounds

containing a second organic bridging ligand, including pyrazine or 4,4′-bipyridine [36,37]. Open-frameworks were constructed in the two compounds under the help of the second organic bridging ligands.

The present study reports on the syntheses and structures of a new family of sodium aluminodiphosphonates, as well as the phenomenal observations of relationships between synthetic conditions and crystal morphologies. As a distinctive structural feature, all crystals presented here possess hexagonal rings and propeller-like chiral motifs in their structures. It is interesting to note that AlMepO-β and AlMepO-α also form channels with methyl groups protruding into these channels, and the size of their channels seems to match properly the cavity size of the title compound [38,39]. Though the structure and the composition are different, a feature common to these crystals is that there are six octahedral aluminium centres at the corner of the hexagonal ring. The large sub-building units may be contributed to the formation of the multi-member ring. An evident goal for the future is to design large sub-building units to construct large open-framework directly, without resorting to the template-assisted method, because the template encapsulated in the structure of inorganic–organic hybrids are very difficult to remove thoroughly. The idea is supported by the work of Yaghi et al., in which large anion units of organic ligands were used to form large open-frameworks [40,41].

2. Experimental procedure

2.1. SEM image and energy-dispersive X-ray (EDX) point analysis

The SEM images were obtained by a JSM-5600LV at 12 kV. The EDX point analysis was performed using an Oxford Instruments X-ray Microanalysis 1350 with an accelerating voltage of 20.00 kV and a system resolution of 77 eV. $Na_2O \cdot Al_2O_3 \cdot 6SiO_2$ (albite), Al_2O_3 (aluminium oxide), and GaP (gallium phosphide) were used as standards for Na, Al, and P, respectively.

2.2. NMR spectra

The ^{13}C CP/MAS, ^{31}P and ^{27}Al MAS NMR were recorded at room temperature on a Bruker DRX-400 spectrometer using a BBO MAS probe with resonance frequencies of 128.4 MHz for ^{13}C, 161.9 MHz for ^{31}P, and 104.3 MHz for ^{27}Al. The magnetic field was 9.4 T. The spin rate of the sample was 4, 6, 8 kHz and the number of scans was 2084, 100, and 100 for ^{13}C, ^{31}P, and ^{27}Al, respectively. The chemical shifts were referenced to the saturated aqueous solution of sodium 4,4-dimethyl-4-silapentane sulfonate (DSS) for ^{13}C, 85% H_3PO_4 for ^{31}P, and 1 M aqueous of aluminium nitrate for ^{27}Al.

2.3. Crystallographic data collection and structure determination

Unit cell parameters and intensity data were determined by using a Bruker Smart 1000 with graphite monochromated Mo-Kα ($\lambda = 0.71073$ Å) radiation at 293 K. The crystal structures were solved by the direct method and refined against F^2 using the SHELXTL software package. The hydrogen atoms were geometrically placed.

2.4. X-ray thermodiffractometric study

The X-ray thermodiffractometric study was performed on a D/MAX-b X-ray diffractometer with Cu Kα radiation ($\lambda = 1.5206$ Å) and operated at 40 and 100 mA. The heating rate was 5 K/min. Prior to the measurements, the samples were hold at different temperatures for 10 min.

2.5. Materials and syntheses

All chemicals used herein were analytical grade and used without further purification.

2.6. DLES-Alt ($C_2H_{19}Al_{0.33}Na_{2.33}O_{14.16}P_2$ with hexagonal tubular morphology)

DLES-Alt was synthesised by a starting reaction gel with a molar composition of 0.15AlOOH (pseudo-boehmite): $0.75Na_4C_2H_4O_7P_2$ (tetra sodium 1-hydroxyethylidenediphosphonate): $0.15Si(OC_2H_5)_4$

(tetraethyl orthosilicate): $3H_2O$ (deionised water): $0.27C_2H_8N_2$ (ethylenediamine): $0.02C_4H_8O_2$ (1,4-dioxane). The mixture was stirred at 303 K until homogeneous, transferred to a 200 ml Teflon-lined stainless autoclave, and then heated at 433 K for 15 days under autogeneous pressure. DLES-Alt was obtained as the major phase adhered to the inner wall of the autoclave, together with unknown sedimentary deposits in the bottom of the autoclave. DLES-Alt crystals were carefully collected from the inner wall. The crystals were washed with ethanol for three times and dried at 313 K. (EDX point analysis: Found Na 12.88, Al 1.84, P 14.51; Calculated Na 13.58, Al 2.26, P 15.71 wt%.)

2.7. DLES-Alts ($C_2H_{16.50}Al_{0.33}Na_3O_{13.25}P_2$ with hexagonal solid morphology)

During the syntheses of DLES-Alt, when the reaction time was altered to 7 days, a small amount of crystals with the solid (herein solid means tubeless) morphology was found to accompany the DLES-Alt. The crystal was designated as DLES-Alts (EDX point analysis: Found Na 17.04, Al 1.86, P 16.48; Calculated Na 17.57, Al 2.27, P 15.78 wt%).

2.8. DLES-Als ($C_2H_{19.67}Al_{0.33}Na_{2.33}O_{14.50}P_2$ with hexagonal solid morphology)

DLES-Als was synthesised by using $Al(i\text{-}OC_3H_7)_3$ (aluminium isopropoxide) or Al (aluminium powder) as the starting material and keeping the same molar ratios and synthetic process for DLES-Alt. (EDX point analysis: Found Na 13.18, Al 1.83, P 14.67; Calculated Na 13.38, Al 2.22, P 15.47 wt%.)

2.9. DLES-Alp ($C_2H_{19.05}Al_{0.33}Na_{2.33}O_{14.19}P_2$ with plate-like solid morphology)

DLES-Alp was a minor crystalline phase, accompanying the major phase of DLES-Alt and DLES-Als. (EDX point analysis: Found Na 12.95, Al 2.33, P 15.77; Calculated Na 13.56, Al 2.25, P 15.67 wt%.)

3. Results and discussion

3.1. Correlation between the synthetic condition and the crystal morphology

Without tetraethyl orthosilicate in the starting materials, small crystals of DLES-Alt could be obtained. DLES-Alt was characterised by powder X-ray diffraction and showed a good crystalline pattern, with the first peak at $d = 15.4652$ Å. Many attempts had been tried to synthesise large single crystals. During the course, it was found that adding tetraethyl orthosilicate into the starting materials favoured the forming of large single crystals of DLES-Alt. It seems that increasing the viscosity of the synthetic system or forming a metastable intermediate of aluminosilicate or silicoaluminodiphosphonate can contribute to the formation of large single crystals. DLES-Alt crystals exhibit hollow hexagonal morphology with conical ends, as shown in Fig. 1(a). The tubes, also hexagonal, could be clearly observed in large DLES-Alt crystals. Typically, DLES-Alt was about 0.05 mm thick and up to 2 mm long.

The following phenomenal discussion on the correlation between the synthetic condition and the crystal morphologies are based on synthetic process for DLES-Alt and tetraethyl orthosilicate was included in the starting materials.

The following describes the effects of reaction times involved the samples obtained separately at different reaction times. Once the reaction was

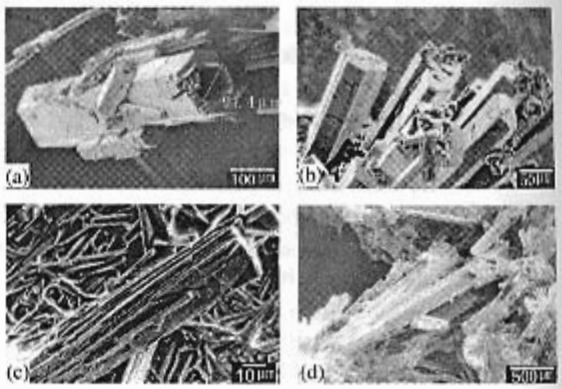

Fig. 1. SEM images of DLES-Alt (a), DLES-Alts (b), DLES-Alp (c) and DLES-Als (d).

interrupted, no follow-up change appeared. If the reaction time was shorter than 2 days, no crystal product was observed (examined by XRD). After 4 days, small DLES-Alt and another two crystals with solid and plate-like morphologies were observed simultaneously (evaluated by microscope). The two crystals were DLES-Alts and DLES-Alp, respectively. Subsequently, the longer the reaction time, the larger the above three crystals. If the reaction time exceeded 7 days, DLES-Alts and DLES-Alp became fewer and fewer, while DLES-Alt turned into the major phase gradually. Figs. 1(b) and (c) show the morphologies of DLES-Alts and DLES-Alp, respectively. For DLES-Alt, the longer the reaction time, the larger the crystal with the larger coaxial hexagonal tubes. All the crystals in our case displayed perfect morphologies, which was different from the Zheng et al.'s results on tubular crystal of Sb_2E_3 [19]. They observed poorly complete tubular crystals and some obvious patch-like bulges.

Used aluminium isopropoxide or aluminium powder as the starting material, another solid crystal (DLES-Als) accompanied by DLES-Alp could be obtained which is illustrated in Fig. 1(d).

To explore the impacts of alkylamine on the crystal morphologies and structures, we used different kinds of alkylamine to replace the ethylenediamine in the starting materials, while keeping the same molar ratio and reaction conditions for DLES-Alt. Seven kinds of alkylamines have been used, including iso-proplamine (C_3H_9N), 1,2-propanediamine ($C_3H_{10}N_2$), butylamine ($C_4H_{11}N$), cyclohexylamine ($C_6H_{13}N$), triethylamine ($C_6H_{15}N$), and triethanolamine ($C_6H_{15}O_3N$). The crystal morphologies of products followed the same transforming processes as that of DLES-Alt. Furthermore, the XRD patterns of the as-synthesised materials were consisted with that of DLES-Alt. That is, alkylamines have no any effects on the crystal morphologies and their structures. The results are supported by the following description of the crystal structures. Namely, although ethylenediamine is one of the starting materials, no ethylenediamine molecules were found in the crystal structure. However, one thing should be emphasised that if no alkylamine was in the starting materials, no DLES-Alt or any other its isostructural crystals was observed.

At present, owing to the appearance, in whatever case, of the plate-like crystals of DLES-Alp and the lamellar crystal structures containing hexagonal rings described herein below, Zheng et al.'s mechanism of the wrapping of sheets of layered compounds seems a reasonable one for explaining the growth mechanism of DLES-Alt [19].

Summarily, the reaction time and aluminium sources have great effects on the crystal morphologies. Contrastively, although the alkylamines are indispensable for synthesising DLES-Alt and its isostructural crystals, they have no impact on the crystal morphologies and their structures.

3.2. Descriptions of the crystal structures

Comprehensively, these sodium aluminodiphosphonates possess a layered structure parallel to the *ab* plane, in which six-coordinate aluminium centres are sharing the vertices with the $\{P(C)O_3\}$ tetrahedron, and are connected together by –O–Na–O–Na–O– ionic chains to form the hexagonal ring. As illustrated by Fig. 2(a), the edge length of the hexagonal ring is approximately 11 Å (calculated by the distance between the two aluminium atoms in one side) and the distance between the two opposite methyl groups are approximately 10 Å. All the above calculations are based on the prime structure with bound water molecules present in the rings. Crystallographic data for compounds DLES-Alt, DLES-Alp, DLES-Alts, and DLES-Als are listed in Table 1.

The compound DLES-Alt is chosen to represent the isostructural series for a detailed structural description. In Table 2, the atomic coordinates and the equivalent isotropic displacement parameters of DLES-Alt are listed.

Fig. 2(b) illustrates the hexagonal channels and a propeller-type environment around the aluminium centre, being viewed along the *c*-axis. The chiral propeller-like motifs are formed by an aluminium-centred octahedron with three six-member cycles. The O–Al–O bond angles for the three blades of the propeller are all equal to 92.39°. These chiral motifs are connected by

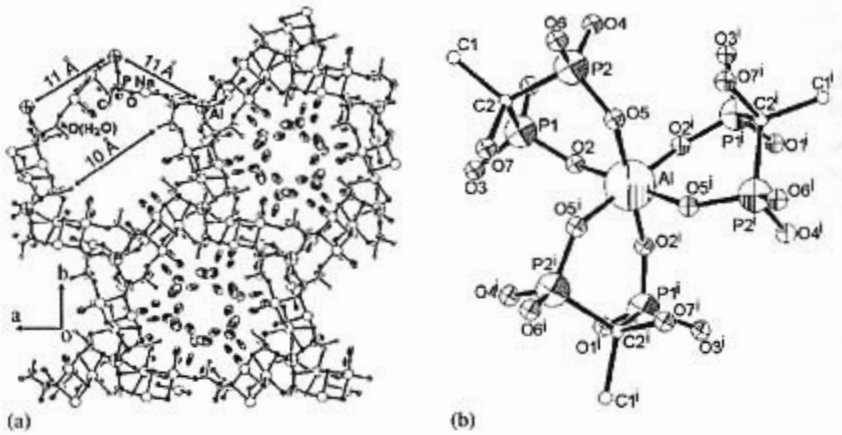

Fig. 2. (a) ORTEP representation of DLES-Alt structure along [0 0 1] and (b) Propeller-type environment around the aluminium centre along [0 0 1]. (Thermal ellipsoids are drawn at 60% probability and hydrogen atoms are omitted for clarity. *i*: equivalent atom. Legends for elements are labelled in figure.)

Table 1
Crystallographic data for compounds DLES-Alt, DLES-Alp, DLES-Alts, and DLES-Als

	DLES-Alt	DLES-Alp	DLES-Alts	DLES-Als
Empirical formula	$C_2H_{19}Al_{0.33}Na_{2.33}O_{14.16}P_2$	$C_2H_{19.05}Al_{0.33}Na_{2.33}O_{14.19}P_2$	$C_2H_{16.50}Al_{0.33}Na_3O_{13.25}P_2$	$C_2H_{19.67}Al_{0.33}Na_{2.33}O_{14.9}P_2$
Formula weight	394.31	394.87	392.56	400.42
Space group	Trigonal	Trigonal	Trigonal	Trigonal
Crystal system	P-3	P-3	P-3	P-3
Cell dimensions: a (Å)	17.853 (4)	17.776 (4)	17.867 (4)	17.981 (6)
b (Å)	17.853 (4)	17.776 (4)	17.867 (4)	17.981 (6)
c (Å)	8.823 (4)	8.798 (4)	8.837 (4)	8.876 (4)
α (deg)	90	90	90	90
β (deg)	90	90	90	90
γ (deg)	120	120	120	120
V (Å^3)	2435.3 (14)	2407.8 (13)	2443.0 (15)	2485.3 (17)
Z	6	6	6	6
Calculated density (Mg/m^3)	1.613	1.634	1.601	1.605
μ (cm^{-1})	0.409	0.414	0.420	0.404
R and $w^a R_2$ [$I > 2\sigma(I)$]	0.0652 and 0.1207	0.0628 and 0.1749	0.0724 and 0.1253	0.0534 and 0.1355
R and $w^a R_2$ (for all data)	0.1539 and 0.1480	0.1101 and 0.2030	0.1648 and 0.1520	0.0822 and 0.1565
Weighting scheme	[a]	[b]	[c]	[d]

[a] $W = 1/(\sigma^2(F_o^2) + (0.0500P)^2 + 0.00P)$, $P = (\max(F_o^2, 0) + 2F_c^2)/3$.
[b] $W = 1/(\sigma^2(F_o^2) + (0.1277P)^2 + 0.00P)$, $P = (\max(F_o^2, 0) + 2F_c^2)/3$.
[c] $W = 1/(\sigma^2(F_o^2) + (0.0500P)^2 + 0.00P)$, $P = (\max(F_o^2, 0) + 2F_c^2)/3$.
[d] $W = 1/(\sigma^2(F_o^2) + (0.0853P)^2 + 3.25P)$, $P = (\max(F_o^2, 0) + 2F_c^2)/3$.

O–Na(2)–O–Na(3)–O ionic chains to form a hexagonal ring. The connected hexagonal rings form two-dimensional layer parallel to the *ab* plane.

Based on the fragment of DLES-Alt along [0 0 1] shown in Fig. 3(a), the crystal structure of DLES-Alt is discussed in detail as follows. All the mentioned NMR spectra herein below are shown in Appendix A. The $-CH_3$ and the neighbouring coordinated water molecule are protruding into the channels. Interestingly, instead of the ethylenediamine molecules, the water molecules lie in the channels. This is verified by ^{13}C CP/MAS NMR of the as-synthesised DLES-Alt, which showed two peaks at 18.8 and 71.3 ppm, assigned to methyl and quaternary carbon atoms, respectively. At the

corner of the hexagon, a six-coordinated aluminium center, sharing vertices with $\{P(C)O_3\}$ tetrahedron and sodium coordinating polyhedron, brings about the hexagonal ring. The sharp symmetrical ^{27}Al MAS NMR resonance at −10.0 ppm supports the assignment of the six-coordinated aluminium. The two phosphorus atoms are all tetrahedrally surrounded by three oxygen atoms and one carbon atom having only one terminal P(2)–O(6) double bond, which is shown in Fig. 3(a). The length of the terminal P=O bond is 1.513 Å. The bond length is between 1.505 and 1.538 Å, longer than that of the H_4hedp [30–32,42,43], because there are strong hydrogen bonds between the P=O and the water molecules trapped between the layers. In addition to the different coordinating environments produced by the sodium atoms, the double bond of P(2)–O(6) increases the weight of the asymmetrical nuclear magnetic field of phosphorus, which is in agreement with the results of ^{31}P MAS NMR (specifically, the two overlapping signals at 18.9 and 20.3 ppm). Na (2) and Na (3) are linking together through an oxygen atom to form an ionic chain lying in the middle of the hexagonal edge. The ionic chains connect the chiral propeller-like motifs together forming the large hexagonal rings. In addition, Na (1) also helps to join the above ionic chains units together.

DLES-Alt, DLES-Als and DLES-Alp exhibit very similar structures. Overall, the crystal structure of DLES-Alts bear strong resemblance to that of DLES-Alt. However, a close examination of the sodium atoms lying in the structure reveals the

Table 2
Atomic coordinates ($\times 10^4$) and equivalent isotropic displacement parameters ($Å^2 \times 10^3$) of refined atoms for DLES-Alt

	x	y	z	U (eq)
P(1)	5289(1)	7780(1)	8807(2)	20(1)
P(2)	4902(1)	6504(1)	11374(1)	19(1)
Al(1)	3333	6667	10065(3)	17(1)
Na(1)	3333	6667	6519(4)	32(1)
Na(2)	4458(1)	5802(2)	7785(2)	34(1)
Na(3)	3877(1)	4289(1)	10614(2)	33(1)
O(1)	6534(3)	7969(4)	10968(7)	33(1)
O(2)	5555(3)	7635(3)	10765(5)	20(1)
O(1)	5617(2)	7344(2)	7748(4)	30(1)
O(2)	4295(2)	7293(2)	8737(4)	24(1)
O(3)	5639(2)	8732(2)	8526(4)	28(1)
O(4)	5029(2)	5926(2)	10294(4)	26(1)
O(5)	3966(2)	6338(2)	11327(4)	20(1)
O(6)	5140(2)	6438(2)	12995(4)	25(1)
O(7)	5361(2)	8172(2)	11760(4)	25(1)
O(8)	3861(3)	5836(3)	5343(4)	40(1)
O(9)	5447(3)	5366(2)	6792(4)	43(1)
O(10)	2979(3)	2857(3)	12087(5)	62(1)
O(11)	3488(3)	3709(3)	5935(6)	71(2)
O(12)	2224(3)	4372(3)	4931(5)	57(1)
O(13)	6551(4)	9118(3)	3939(5)	75(2)
O(14)	1453(8)	1350(9)	1040(20)	150(7)
O(15)	7726(12)	8861(16)	4480(20)	163(9)
O(16)	7602(16)	9364(16)	7500(30)	108(8)

[a] U (eq) is defined as one-third of the trace of the orthogonalised U_{ij} tensor.

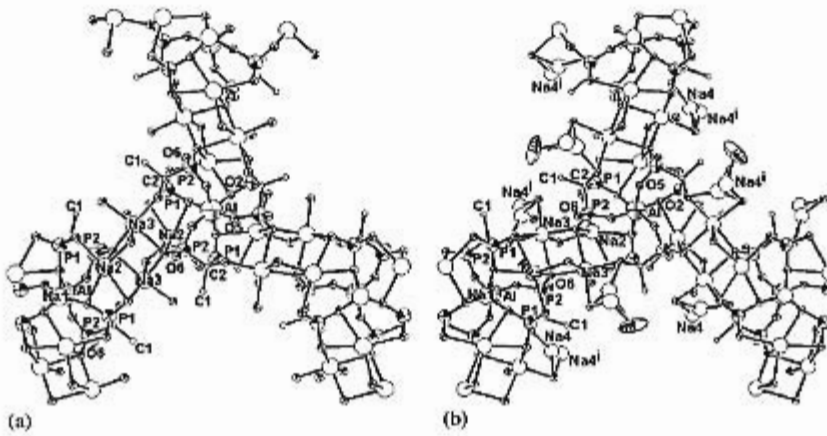

Fig. 3. The fragment of DLES-Alt (a) and DLES-Alts (b) along [0 0 1]. (Thermal ellipsoids are drawn at 60% probability and hydrogen atoms are omitted for clarity. i: equivalent atom. Legends for elements are labelled in figure.)

differences. Comparing Figs. 3(a) and (b), one may find that there are additional sodium ions [Na(4) and its equivalent atoms Na(4^{i})] distributing along the hexagonal channels. Na(4) and its equivalent atoms replaced part of the water molecules linking with the α–O atoms [O(7)] and the coordinated water molecules [O(10), O(11), O(12), and O(15)]. The sodium ions, as well as the protonated water molecules, supply positive charges to balance the negative charges of the framework.

By contrasting the crystallographic data of DLES-Alt and its isostructural crystals, the order of cell dimension is DLES-Als > DLES-Alts > DLES-Alt > DLES-Alp. The crystals with the solid morphology possess larger cell dimensions than the tubular and plate-like crystals.

Based on the above descriptions of the crystal structures, a conclusion could be drawn that water molecules play an important role in the structure. First, the protonated water molecules lying in the channels can balance the negative charges of the framework. Second, water molecules trapped between the layers interact with the terminal oxygen attached to the P atoms through hydrogen bonds, thus forming a stable structure.

Sergienko et al. reviewed the roles of the crystal structural of hedp ions in crystals and found that sodium coordinates the oxygen atom of the α-hydroxy group (α–O atom) without deprotonation. Meanwhile, the α–O atoms bound to Mo(VI) or W(VI) cations are deprotonated in all cases [30,31]. The assignments are based on the crystallographic data. Zheng et al. proposed the protonation of the α–O atom by the evidence of infrared spectra. In our case, with crystal water molecules in the sample, it is very difficult to judge the state of the α-hydroxy group, and further work should be done to answer the question, namely, whether the α-hydroxy group is deprotonated or not? Neutron diffraction should be very useful to solve the problem.

In addition, the thermal stabilities of the crystal structure of DLES-Alt and DLES-Als were evaluated by the thermodiffractometric investigations, and similar results were obtained. Fig. 4 represented the results obtained from DLES-Alt. It is observed that the crystal structure of DLES-Alt is stable up to 343 K. After 373 K, dehydration leads to amorphisation of the products. In view of the layered structure linked together by hydrogen bonds, it is not surprising that they show poor thermal stabilities. A further exploration should be focused on exploring a suitable coupling agent to improve the stability of the layered structure and investigating the possibility of forming tubular morphology by the stabilised structure so obtained.

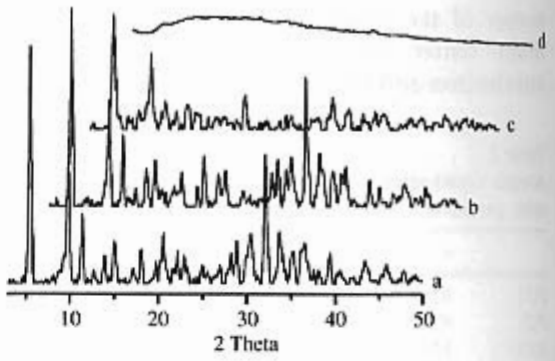

Fig. 4. Thermodiffractometric measurements showing the thermal stability of the structure of DLES-Alt. (a) 293 K, (b) 323 K, (c) 343 K and (d) 373 K.

4. Conclusion

In summary, we have examined four isostructural crystals in the present study, and observed that the reaction conditions have great effects on the crystal morphologies. DLES-Alt is the first reported inorganic–organic hybrid crystal with an interesting tubular morphology. The common structural characteristics for the four layered crystals are hexagonal channels along [0 0 1], and propeller-like chiral units. They are the first example of aluminodiphosphonate with such structures. Moreover, the obtained result supports our claim that layered inorganic–organic hybrid crystals would be potential sources for preparing novel tubular materials.

Acknowledgements

The authors are grateful to the support of the Knowledge Innovation Program of the Chinese Academy of Sciences (Grant: DICP K2000B3).

Appendix A

Spectra of ^{13}C CP/MAS NMR, ^{27}Al MAS NMR, and ^{31}P MAS NMR DLES-Alt are shown in supplementary material. Crystallographic data for the structures reported in this paper have been deposited with the Cambridge Crystallographic Data Centre: CCDC 198391 for DLEA-Alt, CCDC 223468 for DLES-Alts, CCDC 223467 for DLES-Alp, CCDC 198392 for DLES-Als.

References

[1] M. Rosff, Nano-Surface Chemistry, Marcel Dekker Inc., New York, Basel, 2002.
[2] G.R. Patzke, F. Krumeich, R. Nesper, Angew. Chem. Int. Ed. 41 (2002) 2446.
[3] D.T. Bong, T.D. Clark, J.R. Granja, M.R. Ghadiri, Angew. Chem. Int. Ed. 40 (2001) 988.
[4] S. Mann, Angew. Chem. Int. Ed. 39 (2000) 3392.
[5] A. Hirsch, Angew. Chem. Int. Ed. 41 (2002) 1853.
[6] T.F. Betas, L.B. Sand, J.F. Mink, Science 111 (1950) 512.
[7] S. Iijima, Nature 354 (1991) 56.
[8] H.-P. Lin, Ch.-Y. Mou, Science 273 (1996) 765.
[9] M.E. Spahr, P.S. Bitterli, R. Nesper, O. Haas, P. Novák, J. Electrochem. Soc. 146 (1999) 2780.
[10] T. Kasuga, M. Hiramatsu, A. Hoson, T. Sekino, K. Niihara, Langmuir 14 (1998) 3160.
[11] R.Y. Hacohen, E. Grunbaum, R. Tenne, J. Sloan, J.L. Hutchison, Nature 395 (1998) 336.
[12] R.-F. Shen, F.-Y. Wang, Zh.-X. Xiong, R. Xue, Acta Phys. Chim. Sin. 17 (2001) 824.
[13] W.B. Hu, et al., Appl. Phys. A. 70 (2000) 231.
[14] R. Lauterbach, W. Schnick, J. Mater. Sci. 35 (2000) 3793.
[15] R. Sen, B.C. Satishkumar, A. Govindaraj, K.R. Harikumar, G. Raina, J.-P. Zhang, A.K. Cheetham, C.N.R. Rao, Chem. Phys. Lett. 287 (1998) 671.
[16] A.P. Purdy, S. Case, C. George, Crystal Growth Des. 3 (2003) 121.
[17] L.N.S. Oviedo, A.G. Herrero, A.R.L. Cánovas, L.C.O. Díaz, Micron 31 (2000) 597.
[18] R. Tenne, L. Margulis, M. Genut, G. Hodes, Nature 360 (1992) 444.
[19] X.-W. Zheng, Y. Xie, L.-Y. Zhu, X.-Ch. Jiang, Y.-B. Jia, W.-H. Song, Y.-P. Sun, Inorg. Chem. 41 (2002) 455.
[20] J.-Q. Hu, B. Deng, Q.-Y. Lu, K.-B. Tang, R.-R. Jiang, Y.-T. Qian, G.-En. Zhou, H. Cheng, Chem. Commun. (2000) 715.
[21] Ch.-R. Wang, K.-B. Tang, Q. Yang, Sh.-H. Lu, G.-En Zhou, F.-Q. Li, W.-Ch. Yu, Y.-T. Qian, J. Crystal Growth 226 (2001) 175.
[22] A.G. Herrero, A.R.L. Cánovas, S.H. Sen, L.C.Q. Díaz, Micron 31 (2000) 587.
[23] Ch.-R. Wang, K.-B. Tang, Q. Yang, H. Bin, G.-Zh. Shen, Y.-T. Qian, Chem. Lett. (2001) 494.
[24] D. Bernaerts, S. Amelinckx, G.V. Tendeloo, J.V. Landuyt, J. Crystal Growth 172 (1997) 433.
[25] J. Kong, H.T. Soh, A.M. Cassell, C.F. Quate, H.J. Dai, Nature 395 (1998) 878.
[26] S. Amelinckx, X.B. Zhang, D. Bernaerts, X.F. Zhang, V. Ivanov, J.B. Nagy, Science 265 (1994) 635.
[27] J. Portier, J.H. Choy, M.A. Subramanian, Int. J. Inorg. Mater. 3 (2001) 581.
[28] G. Alberti, M. Casciola, U. Costantino, R. Vivani, Adv. Mater. 8 (1996) 291.
[29] A. Clearfield, Prog. Inorg. Chem. 47 (1998) 371.
[30] V.N. Serezhkin, L.B. Serezhkina, V.S. Sergienko, Russ. J. Inorg. Chem. 45 (2000) 521 (and references therein).
[31] V.S. Sergienko, Russ. J. Inorg. Chem. 45 (2000) 1671 (and references therein).
[32] L.-M. Zheng, H.-H. Song, X.-Q. Xin, Comments Inorg. Chem. 22 (2000) 129 (and references therein).
[33] K.L. Nash, R.D. Rogers, J. Ferraro, J. Zhang, Inorg. Chem. Acta. 269 (1998) 211.
[34] P.J. Zapf, D.J. Rose, R.C. Haushalter, J. Zubieta, J. Solid State Chem. 125 (1996) 182.
[35] P. Yin, S. Gao, L.M. Zheng, X.X. Xin, Chem. Mater. 15 (2003) 3233.
[36] P. Yin, L.-M. Zheng, S. Gao, X.-Q. Xin, Chem. Commun. (2001) 2346.
[37] L.-M. Zheng, P. Yin, X.-Q. Xin, Inorg. Chem. 41 (2002) 4084.
[38] K. Meada, J. Akimoto, Y. Kiyozumi, F. Mizukami, Chem. Commun. (1995) 1033.
[39] K. Meada, J. Akimoto, Y. Kiyozumi, F. Mizukami, Angew. Chem. Int. Ed. 34 (1995) 1199.
[40] M. Eddaoudi, J. Kim, N. Rosi, D. Vodak, J. Wachter, M. O'keeffe, O.M. Yaghi, Science 295 (2002) 469.
[41] B.L. Chen, M. Eddaoudi, S.T. Hyde, M. O'keeffe, O.M. Yaghi, Science 291 (2001) 1021.
[42] V.A. Uchtman, R.A. Gloss, J. Phys. Chem. 76 (1972) 1298.
[43] B.L. Barnett, L.C. Strickland, Acta Crystallogr. B 35 (1979) 1212.